

# Limited influence of climate change mitigation on short-term glacier mass loss

Ben Marzeion<sup>1</sup>✉, Georg Kaser<sup>2</sup>, Fabien Maussion<sup>2</sup> and Nicolas Champollion<sup>1</sup>

**Glacier mass loss is a key contributor to sea-level change<sup>1,2</sup>, slope instability in high-mountain regions<sup>3,4</sup> and the changing seasonality and volume of river flow<sup>5–7</sup>. Understanding the causes, mechanisms and time scales of glacier change is therefore paramount to identifying successful strategies for mitigation and adaptation. Here, we use temperature and precipitation fields from the Coupled Model Intercomparison Project Phase 5 output to force a glacier evolution model, quantifying mass responses to future climatic change. We find that contemporary glacier mass is in disequilibrium with the current climate, and  $36 \pm 8\%$  mass loss is already committed in response to past greenhouse gas emissions. Consequently, mitigating future emissions will have only very limited influence on glacier mass change in the twenty-first century. No significant differences between 1.5 and 2 K warming scenarios are detectable in the sea-level contribution of glaciers accumulated within the twenty-first century. In the long-term, however, mitigation will exert strong control, suggesting that ambitious measures are necessary for the long-term preservation of glaciers.**

On time scales of many millennia and longer, glaciers are shaped through interactions with their bedrock<sup>8–10</sup>. On millennial and shorter time scales, their geometry is an expression of the atmospheric conditions surrounding them<sup>11,12</sup>: positive mass balances lead to an expansion of the glacier to lower terminus elevations, while negative mass balances lead to a retreat of the glacier to higher terminus elevations. This mechanism provides a negative feedback<sup>13</sup> through which glaciers adjust their elevation–area distribution to the atmospheric forcing. However, the signal of a perturbed mass balance is distributed over the glacier at a finite velocity, which results in a lagged response of the glacier length to changes in mass balance forcing<sup>14,15</sup>. During periods when climate change is happening rapidly relative to glaciers' response times, glaciers may therefore experience a strong disequilibrium with climate conditions<sup>16</sup>. The amount of ice stored in glaciers<sup>17,18</sup> at any given time may therefore contain a substantial fraction that is not sustainable under current climate conditions.

To quantify this disequilibrium, we first estimate the glacier mass that is sustainable under different global mean temperatures. Note that the spatial distribution of glaciers relative to the spatial pattern of atmospheric temperature change implies that glaciers on average experience higher atmospheric temperature changes than the global mean<sup>13</sup>. We consider all glaciers globally, but exclude peripheral glaciers in Greenland and Antarctica, as well as the ice sheets. Using anomaly fields of temperature and precipitation obtained from the Coupled Model Intercomparison Project Phase 5 (CMIP5) model ensemble and gridded climate observations from the period 1961 to 1990 (refs <sup>19,20</sup>), we force a global glacier evolution model to quantify

the long-term response of each glacier contained in the Randolph Glacier Inventory (RGI) version 5 (ref. <sup>21</sup>), which provides initial surface area and elevation distribution values, to these anomaly fields. This is achieved by repeatedly applying identical climate forcing, corresponding to a given global mean temperature change, to each glacier, until the volume change of the glacier becomes negligible (see Methods for details of the setup of the experiment). The results shown in Fig. 1 indicate a strong disequilibrium between the present-day global glacier mass and present-day climate conditions (when referring to present-day glacier mass, we refer to the year 2015; for present-day climate conditions, we refer to the mean over the years 2006 to 2015), consistent with current in situ observations of glacier mass change<sup>22</sup>. While our estimate of present-day glacier mass is  $307 \pm 18$  mm sea-level equivalent (SLE; the uncertainty indicates the 90% confidence interval), the sustainable ice mass is estimated to 195 (173–222) mm SLE (the numbers in brackets indicate the fifth and ninety-fifth percentiles of the glacier model ensemble), indicating that 36 (28–44)% of the present-day ice mass is unsustainable and would melt if the current climate were to remain stable for the coming centuries. This number is close to previous estimates of  $27 \pm 5\%$ <sup>23</sup> (for the reference year 2006) and  $38 \pm 16\%$ <sup>24</sup> (for the reference period 2000–2010) of already committed but not yet realized glacier mass loss obtained from observed accumulation area ratios. To sustain present-day ice mass, the global mean temperature would have to drop to pre-industrial conditions (when referring to pre-industrial, we refer to the mean over the years 1850–1879). This finding is consistent with previous results that indicate glaciers were strongly responding to the end of the preceding, cooler period of the Little Ice Age before anthropogenic warming became the dominant cause of their mass loss in the second half of the twentieth century<sup>25</sup>. Further global warming increases the present-day commitment to future ice mass loss to 159 (115–179) and 191 (139–205) mm SLE for 1.5 and 2 K warming relative to pre-industrial temperatures, respectively. The equilibrium response of glaciers to warming is nonlinear, with decreased sensitivity at higher temperatures, which is explained by the decreasing surface area and mass of glaciers available for melt.

Using an approximated linear relationship between global anthropogenic CO<sub>2</sub> emissions and global mean temperature change of 1,700 Gt CO<sub>2</sub> emissions per 1 K of warming<sup>26</sup>, we calculate the global glacier mass change commitment of CO<sub>2</sub> emissions as a function of the global mean temperature (Fig. 2). Since this mass change commitment is calculated from the equilibrium glacier mass, it is independent of, and in addition to, any potential mass changes committed in the past, but not yet realized. We find that under present-day climate conditions, every emitted kg of CO<sub>2</sub> will eventually be responsible for a glacier mass loss of 15.8 (5.9–20.5) kg. Again, since the global glacier mass is decreasing with increasing temperatures,

<sup>1</sup>Institute of Geography, University of Bremen, Bremen, Germany. <sup>2</sup>Department of Atmospheric and Cryospheric Sciences, Universität Innsbruck, Innsbruck, Austria. ✉e-mail: [ben.marzeion@uni-bremen.de](mailto:ben.marzeion@uni-bremen.de)

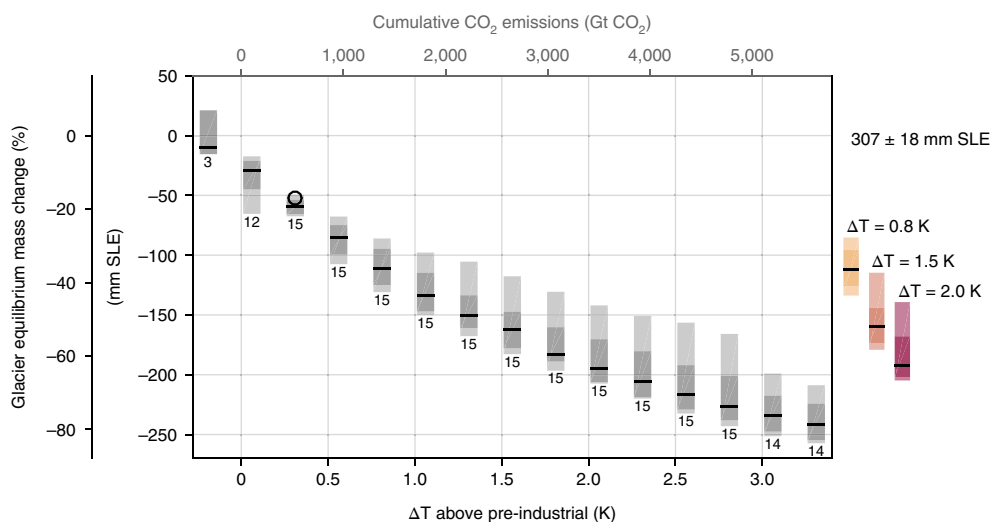


**Fig. 1 | Global glacier equilibrium mass.** Glacier mass is shown as the change relative to present-day (year 2015) mass, as indicated by the number on the upper right corner, and as a function of the global mean temperature change relative to the pre-industrial temperature (1850–1879). Small numbers indicate the size of the glacier model ensemble. Light shading indicates the fifth to ninety-fifth percentile of the ensemble, while dark shading indicates the fifteenth to eighty-fifth percentile. The black line represents the ensemble median. The coloured shading and lines on the right side indicate the glacier equilibrium mass interpolated to different global mean temperatures, including the present-day (2006–2015) air temperature (0.8 K above the pre-industrial temperature). The black ring indicates forcing with climate observations during the period 1961–1990. The upper horizontal axis (anthropogenic cumulative CO<sub>2</sub> emissions) is only approximate.

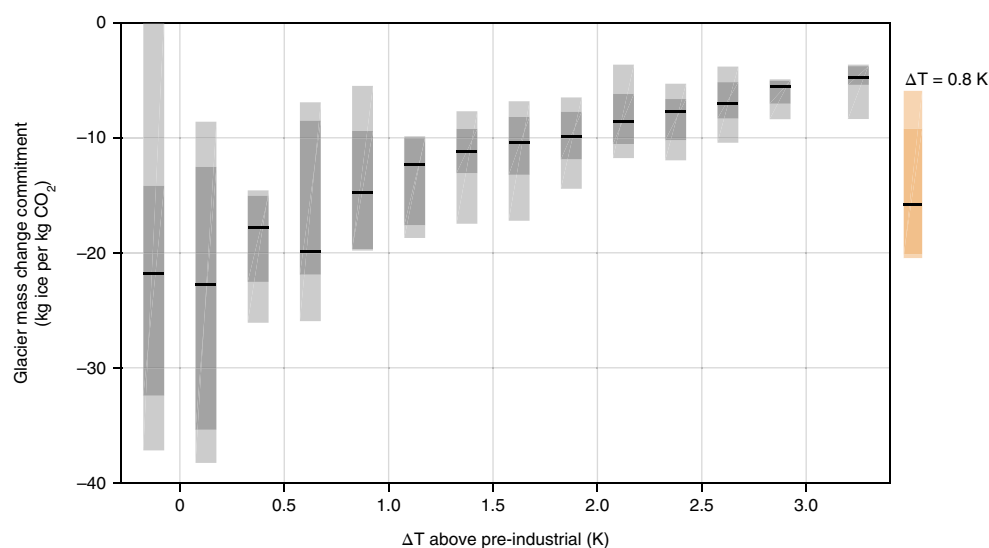


**Fig. 2 | Global glacier mass change commitment as a function of global mean temperature change relative to the pre-industrial (1850–1879) temperature.** Light shading indicates the fifth to ninety-fifth percentile of the glacier model ensemble, while dark shading indicates the fifteenth to eighty-fifth percentile. The black line represents the ensemble median. The coloured shading and the line on the right indicate values interpolated to the present-day (2006–2015) temperature change.

this number is greater for lower temperatures and smaller for higher temperatures.

These results indicate that a large fraction of glacier mass change projected for the twenty-first century<sup>27–30</sup> will be a response to mass change commitments of the past. For example, if the global mean temperature was limited to rise to 1.5 K above pre-industrial values, as envisioned in the Paris Agreement, and kept at this value, about 70% of the eventual glacier mass loss would be the realization of mass loss commitments originating from greenhouse gases emitted before the Paris Agreement. If the warming was limited to, and kept at, 2 K, this number would drop to about 60%.

However, not all of the eventual mass change will be realized within the next century. We update projections of twenty-first century mass change<sup>27</sup> using a more recent glacier inventory (version 5, updated from version 1) and adding projections corresponding to 1.5 and 2.0 K of global mean temperature change above pre-industrial values. Since no CMIP projections dedicated to this goal exist so far, we scale temperature and precipitation anomaly fields from the RCP2.6 ensemble of CMIP5 to derive forcing fields for the glacier model (referred to as 1.5 and 2 K scenarios from here on; see Methods for details). Time series of the resulting global mean temperature anomalies are shown in Fig. 3a. The differences

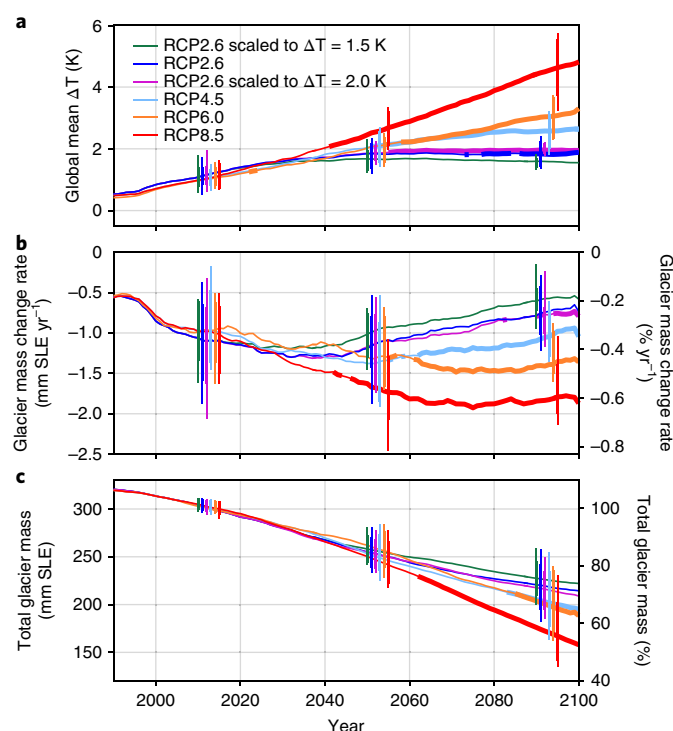


**Fig. 3 | Projections of global glacier mass change.** **a**, Global mean temperature anomalies relative to the pre-industrial (1850–1879) temperature. **b**, Glacier mass change rates. **c**, Global glacier mass. Vertical lines indicate the fifth to ninety-fifth (thin) and fifteenth to eighty-fifth (thick) percentiles of the CMIP5 (**a**) or glacier model (**b** and **c**) ensembles at different times. Time series show the ensemble median. Increased line thicknesses of time series indicate periods with a significant difference from the ensemble scaled to  $\Delta T = 1.5$  K. The time series in **a** and **b** have been smoothed using a 10 year moving average for visual clarity.

between the RCP2.6 ensemble and 1.5 and 2 K scenarios are small. However, a significant difference between the RCP2.6 ensemble and the ensemble scaled to 1.5 K is detectable in the second half of the twentieth century.

In all projections, glacier mass loss accelerates at least until the mid-twenty-first century (Fig. 3b). No significant difference in global glacier mass change is detectable—even between the RCP8.5 and the 1.5 K scenario—until 2040. In the second half of the twenty-first century, for the low-emission scenarios, glaciers strive towards a new equilibrium with climate conditions, expressed by lowering mass loss rates. In the high-emission scenarios, mass loss accelerates well into the second half of the century. No significant difference can be detected between the 1.5 K and RCP2.6 scenarios, and only at the very end of the century between the 1.5 and the 2 K scenarios.

From the present day to the end of the twenty-first century, glaciers are projected to lose 76 (54–97) mm SLE under the 1.5 K scenario, 84 (54–116) mm SLE under the RCP2.6 scenario, 89 (63–112) mm SLE under the 2 K scenario, 104 (58–136) mm SLE under the RCP4.5 scenario, 110 (75–140) mm SLE under the RCP6.0 scenario and 142 (83–165) mm SLE under the RCP8.5 scenario (Fig. 3c). In global glacier mass, no significant difference is detectable within the twenty-first century between the 1.5 K, RCP2.6 and 2 K scenarios. A difference between the 1.5 K scenario and the RCP4.5 and RCP6.0 scenarios only emerges after 2080, and a difference between the 1.5 K and RCP8.5 scenarios only emerges after 2060.

Reductions of greenhouse gas emission will have limited impact on twenty-first century glacier mass loss, as a large fraction of that mass loss and resulting glacier run-off is the realization of past commitments. To a large degree, future glacier mass loss needs to be considered inevitable, making the identification and execution of appropriate adaptation measures mandatory. However, because of the nonlinear nature of global glacier mass sensitivity to global temperature change, more ambitious climate change mitigation measures will have a disproportionately greater impact on the long-term preservation of glaciers than less ambitious measures, reducing the required adaptive measures.

## Methods

Methods, including statements of data availability and any associated accession codes and references, are available at <https://doi.org/10.1038/s41558-018-0093-1>.

Received: 3 November 2017; Accepted: 30 January 2018;

Published online: 19 March 2018

## References

- Gregory, J. M. et al. Twentieth-century global-mean sea-level rise: is the whole greater than the sum of the parts? *J. Clim.* **26**, 4476–4499 (2013).
- Church, J. et al. in *Climate Change 2013: The Physical Science Basis* (eds Stocker, T. et al.) 1137–1216 (IPCC, Cambridge Univ. Press, 2014).
- Richardson, S. D. & Reynolds, J. M. An overview of glacial hazards in the Himalayas. *Quat. Int.* **65**, 31–47 (2000).
- Huggel, C., Clague, J. J. & Korup, O. Is climate change responsible for changing landslide activity in high mountains? *Earth Surf. Process. Landf.* **37**, 77–91 (2012).
- Jansson, P., Hock, R. & Schneider, T. The concept of glacier storage: a review. *J. Hydrol.* **282**, 116–129 (2003).
- Immerzeel, W. W., van Beek, L. P. H. & Bierkens, M. F. P. Climate change will affect the Asian water towers. *Science* **328**, 1382–1385 (2010).
- Huss, M. Present and future contribution of glacier storage change to runoff from macroscale drainage basins in Europe. *Water Resour. Res.* **47**, W07511 (2011).
- Egholm, D., Nielsen, S., Pedersen, V. K. & Lesemann, J.-E. Glacial effects limiting mountain height. *Nature* **460**, 884–887 (2009).
- Thomson, S. N. et al. Glaciation as a destructive and constructive control on mountain building. *Nature* **467**, 313–317 (2010).
- Korup, O., Montgomery, D. R. & Hewitt, K. Glacier and landslide feedbacks to topographic relief in the Himalayan syntaxes. *Proc. Natl Acad. Sci. USA* **107**, 5317–5322 (2010).
- Oerlemans, J. Extracting a climate signal from 169 glacier records. *Science* **308**, 675–677 (2005).
- Kaser, G., Cogley, J. G., Dyurgerov, M. B., Meier, M. F. & Ohmura, A. Mass balance of glaciers and ice caps: consensus estimates for 1961–2004. *Geophys. Res. Lett.* **33**, L19501 (2006).
- Marzeion, B., Jarosch, A. H. & Gregory, J. M. Feedbacks and mechanisms affecting the global sensitivity of glaciers to climate change. *Cryosphere* **8**, 59–71 (2014).
- Jóhannesson, T., Raymond, C. & Waddington, E. Time-scale for adjustment of glaciers to changes in mass balance. *J. Glaciol.* **35**, 355–369 (1989).
- Bahr, D. B., Pfeffer, W. T., Sassolas, C. & Meier, M. F. Response time of glaciers as a function of size and mass balance: 1. Theory. *J. Geophys. Res. Solid Earth* **103**, 9777–9782 (1998).
- Pelto, M. S. The current disequilibrium of North Cascade glaciers. *Hydrol. Process.* **20**, 769–779 (2006).
- Huss, M. & Farinotti, D. Distributed ice thickness and volume of all glaciers around the globe. *J. Geophys. Res.* **117**, F04010 (2012).
- Grinsted, A. An estimate of global glacier volume. *Cryosphere* **7**, 141–151 (2013).
- New, M., Lister, D., Hulme, M. & Makin, I. A high-resolution data set of surface climate over global land areas. *Clim. Res.* **21**, 1–25 (2002).
- Mitchell, T. D. & Jones, P. D. An improved method of constructing a database of monthly climate observations and associated high-resolution grids. *Int. J. Climatol.* **25**, 693–712 (2005).
- Pfeffer, W. T. et al. The Randolph Glacier Inventory: a globally complete inventory of glaciers. *J. Glaciol.* **60**, 537–552 (2014).
- Zemp, M. et al. Historically unprecedented global glacier decline in the early 21st century. *J. Glaciol.* **61**, 745–762 (2015).
- Bahr, D. B., Dyurgerov, M. & Meier, M. F. Sea-level rise from glaciers and ice caps: a lower bound. *Geophys. Res. Lett.* **36**, L03501 (2009).

24. Mernild, S. H., Lipscomb, W. H., Bahr, D. B., Radić, V. & Zemp, M. Global glacier retreat: a revised assessment of committed mass losses and sampling uncertainties. *Cryosphere* **7**, 1565–1577 (2013).
25. Marzeion, B., Cogley, J. G., Richter, K. & Parkes, D. Attribution of global glacier mass loss to anthropogenic and natural causes. *Science* **345**, 919–921 (2014).
26. Stocker, T. et al. in *Climate Change 2013: The Physical Science Basis* (eds Stocker, T. et al.) 33–115 (IPCC, Cambridge Univ. Press, 2014).
27. Marzeion, B., Jarosch, A. H. & Hofer, M. Past and future sea-level change from the surface mass balance of glaciers. *Cryosphere* **6**, 1295–1322 (2012).
28. Giesen, R. H. & Oerlemans, J. Climate-model induced differences in the 21st century global and regional glacier contributions to sea-level rise. *Clim. Dyn.* **41**, 3283–3300 (2013).
29. Bliss, A., Hock, R. & Radić, V. Global response of glacier runoff to twenty-first century climate change. *J. Geophys. Res.* **119**, 717–730 (2014).
30. Huss, M. & Hock, R. A new model for global glacier change and sea-level rise. *Front. Earth Sci.* **3**, 54 (2015).

## Acknowledgements

This work was funded by the German Federal Ministry of Education and Research (grant 01LS1602A) and German Research Foundation (grant MA 6966/1-1), and supported by the Austrian Federal Ministry of Science and Research as part of the UniInfrastrukturprogramm of the research platform Scientific Computing at the University of Innsbruck. We acknowledge the World Climate Research Programme's Working Group on Coupled Modelling, which is responsible for the CMIP, and we

thank the climate modelling groups (listed in Supplementary Table 1) for producing and making available their model output. For the CMIP, the US Department of Energy's Program for Climate Model Diagnosis and Intercomparison provided coordinating support and led development of software infrastructure in partnership with the Global Organization for Earth System Science Portals. We thank R. Stauffer and A. Kreuter for help with the figure design.

## Author contributions

B.M., G.K. and F.M. conceived the study and designed the experiments. B.M. performed the experiments and analysed the results. B.M. and N.C. wrote the manuscript. All authors discussed the results and the manuscript.

## Competing interests

The authors declare no competing interests.

## Additional information

**Supplementary information** is available for this paper at <https://doi.org/10.1038/s41558-018-0093-1>.

**Reprints and permissions information** is available at [www.nature.com/reprints](http://www.nature.com/reprints).

**Correspondence and requests for materials** should be addressed to B.M.

**Publisher's note:** Springer Nature remains neutral with regard to jurisdictional claims in published maps and institutional affiliations.

## Methods

**Glacier model.** The glacier model is set out in full in refs <sup>13,25,27,31</sup>, on which the following description relies heavily. We refer the reader to these sources for further detail.

The glacier model is based on calculating the annual specific climatic mass balance  $B$  for each of the world's individual glaciers as

$$B = \left( \sum_{i=1}^{12} (P_i^{\text{solid}} - \mu \star \max(T_i^{\text{terminus}} - T_{\text{melt}}, 0)) \right) - \beta \star \quad (1)$$

where  $P_i^{\text{solid}}$  is the monthly solid precipitation onto the glacier surface per unit area, which depends on the monthly mean total precipitation and the temperature range between the glacier's terminus and highest elevations (that is, the temperature at terminus elevation below a certain threshold implies all precipitation is solid, the temperature at the glacier's maximum elevation above the threshold implies all precipitation is liquid, and within that temperature range, the precipitation fraction is interpolated linearly),  $\mu$ , is the glacier's temperature sensitivity,  $T_i^{\text{terminus}}$  is the monthly mean air temperature at the glacier's terminus,  $T_{\text{melt}}$  is the monthly mean air temperature above which ice melt is assumed to occur and  $\beta \star$  is a bias correction (see below). The model thus does not attempt to capture the full energy balance at the ice surface, but relies on air temperature as a proxy for the energy available for melt<sup>32–34</sup>.  $P_i^{\text{solid}}$  and  $T_i^{\text{terminus}}$  are determined based on gridded climate observations<sup>19,20</sup>, to which temperature and precipitation anomaly fields from the CMIP5 models are added (see Supplementary Table 1). Changes affecting the glacier hypsometry (that is, changes in its volume, surface area and elevation range) are reflected in the determination of  $P_i^{\text{solid}}$  and  $T_i^{\text{terminus}}$ , which are modelled based on  $B$ , and on linearly adjusting the glacier's surface area and length towards their respective values obtained from volume–area and volume–length scaling<sup>35,36</sup>. That is, the surface area change  $dA$  of a glacier during each mass balance year  $t$  is calculated as

$$dA(t) = \frac{1}{\tau_A(t)} \left( \left( \frac{V(t+1)}{c_A} \right)^{1/\gamma} - A(t) \right) \quad (2)$$

where  $\tau_A(t)$  is the area relaxation time scale (see equation (5)),  $V(t+1)$  is the glacier's volume at the end of the mass balance year,  $c_A = 0.0340 \text{ km}^{3-2\gamma}$  (for glaciers),  $c_A = 0.0538 \text{ km}^{3-2\gamma}$  (for ice caps),  $\gamma = 1.375$  (for glaciers) and  $\gamma = 1.25$  (for ice caps) are scaling parameters<sup>35,36</sup>, and  $A(t)$  is the surface area of the glacier at the end of the preceding mass balance year. Similarly, length changes  $dL$  (and terminus elevation changes associated with them) during each mass balance year are estimated as

$$dL(t) = \frac{1}{\tau_L(t)} \left( \left( \frac{V(t+1)}{c_L} \right)^{1/q} - L(t) \right) \quad (3)$$

where  $\tau_L(t)$  is the length relaxation time scale (see equation (4)),  $c_L = 0.0180 \text{ km}^{3-q}$  (for glaciers),  $c_L = 0.2252 \text{ km}^{3-q}$  (for ice caps),  $q = 2.2$  (for glaciers) and  $q = 2.5$  (for ice caps) are scaling parameters<sup>35,36</sup>, and  $L(t)$  is the glacier's length at the start of the mass balance year. The glacier length response time scale  $\tau_L$  is estimated roughly following ref. <sup>14</sup> as

$$\tau_L(t) = \frac{V(t)}{\sum_{i=1}^{12} \int P_{i,\text{clim}}^{\text{solid}}(t)} \quad (4)$$

where  $\int P_{i,\text{clim}}^{\text{solid}}$  is the monthly climatological solid precipitation integrated over the glacier surface area, calculated over the preceding 30 years. The glacier area response time scale is estimated as

$$\tau_A(t) = \tau_L(t) \frac{A(t)}{L(t)^2} \quad (5)$$

based on the assumption that area changes caused by glacier width changes occur instantaneously, while area changes caused by glacier length changes occur with the time scale of the glacier length response.

The volume change  $dV$  of a glacier in year  $t$  is calculated as

$$dV(t) = B(t) \cdot A(t). \quad (6)$$

The temperature sensitivity  $\mu \star$  is determined from observed past variations for each of the glaciers with available mass balance observations<sup>37,38</sup>. In these datasets, there are a global total of 255 glaciers that have all the metadata needed for the parameter estimation, are covered by the temperature and precipitation dataset we use (see below), are indicated to be reliable and have at least two annual mass balance measurements. The procedure is as follows. We assume that there exists some 31 year reference period, centred on year  $t^\star$ , whose climatology is such that the glacier with its present-day hypsometry would be in equilibrium; that is, with its mass not changing. For this reference period, by construction

$$B = \sum_{i=1}^{12} (P(t^\star)_{i,\text{clim}}^{\text{solid}} - \mu(t^\star) \cdot (\max(T(t^\star)_{i,\text{clim}}^{\text{terminus}} - T_{\text{melt}}, 0))) = 0 \quad (7)$$

where  $P(t^\star)_{i,\text{clim}}^{\text{solid}}$  and  $T(t^\star)_{i,\text{clim}}^{\text{terminus}}$  are the monthly climatological values of  $P_i^{\text{solid}}$  and  $T_i^{\text{terminus}}$ , during the 31 year period centred around the year  $t^\star$ . Note that we do not assume  $t^\star$  to be a time at which the glacier was actually in balance. If the climate has been warming and the glacier retreating—as is generally the case— $t^\star$  would be in the past, and the glacier would actually have had a negative mass balance at time  $t^\star$ . The assumption is that if the climate of time  $t^\star$  had been maintained, the glacier eventually would have contracted until it reached its present-day hypsometry.

We obtain a total of 109 monthly climatologies of precipitation and temperature (the dataset of ref. <sup>20</sup> provides 109 years of monthly precipitation and temperature; at the end and beginning of the time series, the climatologies are calculated over shorter time periods), and subsequently obtain an estimate of  $\mu$  from equation (7) for each of the 109 choices of  $t^\star$ . We then apply the glacier model to all glaciers for which direct mass balance observations are available, for each of the 109 possible values of  $\mu(t)$ . For each of these glaciers, we identify  $t^\star$  as that time, for which applying the corresponding temperature sensitivity  $\mu \star \equiv \mu(t^\star)$  yields the smallest mean error of the modelled mass balances. This minimum difference is denoted by  $\beta \star$ .

For glaciers without observed mass balances (that is, the vast majority of glaciers),  $t^\star$  is interpolated from the ten closest surrounding glaciers with mass balance observations, weighted inversely by distance.  $\mu \star$  is subsequently determined by solving equation (7) for  $\mu \star$ , using precipitation and temperature obtained from the climatology centred around the interpolated value of  $t^\star$ . The bias correction  $\beta \star$  is determined by interpolating the minimized bias obtained during the determination of  $t^\star$  from surrounding glaciers with mass balance observations.

The value of  $\mu \star$  can vary greatly between neighbouring glaciers without obvious physical reasons, depending on glacier-specific issues such as avalanches, topographical shading, cloudiness and other issues related to systematic biases in the input data (for example, climate or topography). By interpolating  $t^\star$  instead of  $\mu \star$  for glaciers without mass balance observations, the constraint of  $\mu(t)$  to not vary much with time is used (1) to take into account the glacier-specific issues mentioned above (that is,  $\mu(t)$  will vary comparatively little around a given year  $t$ ; errors in  $t^\star$ —even large ones—will result in relatively small errors in  $\mu \star$ ) and (2) to help compensate systematic biases in temperature and precipitation data. In that sense, the calibration procedure can be seen as an empirically driven downscaling strategy: if a glacier is located there, the local climate (or the glacier temperature sensitivity) must allow a glacier to be there. For example, the effect of avalanches or a negative bias in precipitation input will have the same impact on calibration: the value of  $\mu \star$  will be lowered to take these effects into account, even though they are not resolved by the mass balance model. A cross-validation of the determination of  $\mu \star$  shows that the spatial interpolation of  $t^\star$  leads to substantially smaller errors than the spatial interpolation of  $\mu \star$ <sup>27</sup>.

Initial values for the surface area and elevation distribution of each glacier are obtained from the Randolph Glacier Inventory version 5. The model accounts for the differing dates of surface area measurement in the Randolph Glacier Inventory by ensuring that the observed glacier extent is reproduced in the year of observation.

Present-day glacier mass is taken as a snapshot in the year 2015 from a transient reconstruction, with the model being forced by gridded climate observations<sup>20</sup>. Uncertainties (as given in Fig. 1) are based on the propagated model uncertainties obtained through the leave-one-glacier-out cross-validation described below (see refs <sup>27,31</sup> for details).

**Validation of the glacier model and treatment of uncertainties.** Uncertainty estimates of the glacier model are obtained by: (1) performing a leave-one-glacier-out cross-validation that allows us to determine the model's performance on glaciers without direct mass balance observations; (2) propagating these uncertainties, and uncertainties of model parameters needed for, for example, the estimation of the initial ice volume, through the entire glacier model; and (3) validating these propagated and temporally accumulated uncertainties themselves, using independent geodetically measured volume and surface area changes<sup>37</sup>. For this second validation, the uncertainty estimates are found to be realistic. The systematic, global mean bias of the glacier model's annual specific glacier-wide mass balance is 5 mm water equivalent (not significantly different from zero).

Given any pair of glaciers for which the cross-validation is carried out, we may calculate the temporal correlation between the annual time series for those two glaciers of the errors in the modelled mass balance. Considering all such pairs, we can calculate the correlation of this temporal error correlation with the distance between the two glaciers. This latter correlation is  $<0.01$  (not significant), indicating that the model errors for the individual glaciers can be treated as independent of each other, irrespective of their distance. The uncertainties for the globally aggregated data are thus obtained by taking the square root of the summed and squared uncertainties of the individual glaciers' results. A more detailed and complete description of the determination of the model's parameters, both glacier-specific and global, and of the comprehensive validation of the model, can be found in ref. <sup>27</sup>.



For scenario-based results, the total uncertainty is strongly dominated by the ensemble spread, not glacier model uncertainty (for example, for the RCP8.5 scenario, the uncertainty of the individual ensemble members is of the order of 5 mm SLE, while the ensemble spread is of the order of 100 mm SLE at the end of the twenty-first century). Uncertainties for these results are therefore given as the fifth to ninety-fifth percentile of the ensemble distribution.

For the equilibrium results, the uncertainties obtained through propagation and temporal accumulation in the glacier model are meaningless, since they are mostly a function of the model integration time. That is, estimating the glaciers' equilibrium mass more accurately by integrating the glacier model for a longer time artificially inflates the propagated model uncertainty. Therefore, uncertainties are again given as the fifth to ninety-fifth percentile of the ensemble distribution in this case.

The uncertainty of the present-day ice mass estimate (Fig. 1) is obtained from the error propagation described above, applied to the glacier model forced by climate observations<sup>30</sup>. The ice mass estimate is slightly higher than an estimate obtained through a more elaborate method<sup>17</sup>, but consistent with it considering the respective uncertainties.

**Equilibrium experiments.** Results from 15 different CMIP5 models, using the historical run continued by the RCP8.5 scenario (see Supplementary Table 1), were used to force the glacier model in the equilibrium experiments over a range of global mean temperature anomalies. The RCP8.5 scenario was chosen to obtain the largest possible ensemble size also for relatively high global mean temperature anomalies.

For each of the combined historical and RCP8.5 experiments, monthly anomaly fields of precipitation and near surface air temperature were determined, relative to the monthly climatology of 1961 to 1990. Then, global mean temperature anomalies were determined for each 30-year period contained in the combined historical and RCP8.5 experiment. From this dataset, we obtained 30-year-long anomaly fields of precipitation and temperature, which correspond most closely to a given global mean temperature anomaly. Since the range of global mean temperature anomalies differs between the different CMIP5 models, the number of anomaly fields extracted from each CMIP5 also differs, leading to an ensemble size that depends on the global mean temperature anomaly considered (small numbers in Fig. 1). The anomaly fields were then added to the observed climatological fields of ref.<sup>19</sup> to obtain the climate forcing for the glacier model. Additionally, the glacier model was forced by the observed climatological fields of ref.<sup>19</sup> only, with temporal variability added from the same period from ref.<sup>20</sup> (black circle in Fig. 1). Note that because of the temperature threshold sensitivity of the mass balance, zero-mean temporal variability also has a net effect on glacier volume, and identical mean temperatures can result in different glacier masses, as a result of different temporal variability. We express all temperature anomalies relative to the global mean temperature averaged between 1850 and 1879 in ref.<sup>39</sup>.

To obtain the equilibrium response of the glaciers to a given global mean temperature forcing, the same forcing (30 years) was repeatedly applied for each glacier until volume changes of the glacier became negligible. This was defined to be the case when the volume change over the past 100 modelled years was smaller than 1% of the glacier volume. Reaching the equilibrium took up to approximately 700 years. On the global scale, ice volume changes are small after 200 years. Note that in an experimental setup like this, glaciers may reach an equilibrium, while the state of the climate system that was used to drive the glaciers into equilibrium is not itself a true equilibrium, but picked from a transient scenario.

To relate global mean temperature anomalies to anthropogenic CO<sub>2</sub> emissions (upper horizontal axis in Fig. 1 and calculations for Fig. 2), we assume a linear relationship between the two based on Fig. TFE 8.1 in ref.<sup>26</sup>. We estimate this relationship to 1 K global mean temperature change per 1,700 Gt CO<sub>2</sub> emissions.

**Transient experiments.** Transient experiments for the RCP2.6, RCP4.5, RCP6.0 and RCP8.5 scenarios were performed exactly as described in ref.<sup>27</sup>, except that the initial conditions for each glacier were updated to the Randolph Glacier Inventory version 5. To obtain scenarios corresponding to 1.5 and 2.0 K of warming, anomalies of CMIP5 RCP2.6 runs were scaled using a time-dependent scaling factor. First, for each considered run, its global mean temperature anomaly during

the period 2071 to 2100 was determined, as well as the associated scaling factor needed to bring it to 1.5 or 2.0 K exactly. Then, starting in 2016 with a scaling factor of 1 (to avoid a discontinuity in the forcing fields), temperature anomaly fields were scaled down (or up), with the scaling factor increasing linearly in time until it reached its pre-determined value at the end of the twenty-first century. This implies that for all scaled model runs, the global mean temperature during the past 30 years of the twenty-first century is exactly 1.5 or 2.0 K above the pre-industrial temperature, which reduces the spread of the scaled model ensemble considerably. However, the temporal and spatial variability of each CMIP5 run is retained. It is unclear how precipitation anomalies should be related from the RCP2.6 scenario to the 1.5 and 2.0 K scenarios. For the results shown here, we applied the same scaling factors used for the temperature anomaly fields to the precipitation anomaly fields based on the assumption that the amplitude of precipitation anomalies is linked to temperature anomalies<sup>40</sup>. While this relationship should not be expected to hold regionally and at all times, it has very minor impacts on our results: to test the sensitivity of our results to this approach, we repeated the projections, leaving the precipitation anomaly fields unscaled. The differences compared with the results presented here were vanishingly small.

An alternative approach to scaling would be the selection of RCP2.6 ensemble members that end up close to the 1.5 or 2.0 K global mean temperature anomaly, as has been done in a regional study<sup>41</sup>. We prefer the scaling approach for two reasons: (1) it does not reduce the ensemble size, leading to more robust uncertainty statistics; and (2) it circumvents the possibility that selecting climate models that have a relatively low (or high) climate sensitivity leads to a reduction in the spread of temporal and spatial climate variability.

To conclude whether the applied model chain is able to distinguish between the 1.5 K and other scenarios, we perform a two-sample Kolmogorov–Smirnov test. For each year, we test at the  $P < 0.05$  level against the null hypothesis that two ensembles—one of them being the 1.5 K scenario—are drawn from the same underlying population.

**Data availability.** The glacier model results and scaled climate projections presented here are available from the corresponding author upon reasonable request.

## References

- Marzeion, B., Leclercq, P., Cogley, J. & Jarosch, A. Brief communication: global reconstructions of glacier mass change during the 20th century are consistent. *Cryosphere* **9**, 2399–2404 (2015).
- Ohmura, A. Physical basis for the temperature-based melt-index method. *J. Appl. Meteorol.* **40**, 753–761 (2001).
- Hock, R. Temperature index melt modelling in mountain areas. *J. Hydrol.* **282**, 104–115 (2003).
- Sicart, J., Hock, R. & Six, D. Glacier melt, air temperature, and energy balance in different climates: the Bolivian tropics, the French Alps, and northern Sweden. *J. Geophys. Res.* **113**, D24113 (2008).
- Bahr, D., Meier, M. & Peckham, S. The physical basis of glacier volume–area scaling. *J. Geophys. Res.* **102**, 355–362 (1997).
- Bahr, D. Global distributions of glacier properties: a stochastic scaling paradigm. *Water Resour. Res.* **33**, 1669–1679 (1997).
- Cogley, J. G. Geodetic and direct mass-balance measurements: comparison and joint analysis. *Ann. Glaciol.* **50**, 96–100 (2009).
- Fluctuations of Glaciers 2005–2010* (World Glacier Monitoring Service, 2012).
- Morice, C. P., Kennedy, J. J., Rayner, N. A. & Jones, P. D. Quantifying uncertainties in global and regional temperature change using an ensemble of observational estimates: the HadCRUT4 data set. *J. Geophys. Res.* **117**, D08101 (2012).
- Andrews, T., Forster, P. M., Boucher, O., Bellouin, N. & Jones, A. Precipitation, radiative forcing and global temperature change. *Geophys. Res. Lett.* **37**, L14701 (2010).
- Kraaijenbrink, P., Bierkens, M., Lutz, A. & Immerzeel, W. Impact of a global temperature rise of 1.5 degrees Celsius on Asia's glaciers. *Nature* **549**, 257–260 (2017).